water

MDPI

Article

In Situ Water Quality Measurements Using an Unmanned Aerial Vehicle (UAV) System

Cengiz Koparan, Ali Bulent Koc *, Charles V. Privette and Calvin B. Sawyer

Department of Agricultural Sciences, Agricultural Mechanization and Business, Clemson University, Clemson, SC 29634, USA; ckopara@g.clemson.ed (C.K.); privett@clemson.edu (C.V.P.); calvins@clemson.edu (C.B.S.)

* Correspondence: bulent@clemson.edu; Tel.: +1-864-656-0496

Received: 9 January 2018; Accepted: 27 February 2018; Published: 3 March 2018

Abstract: An unmanned aerial vehicle-assisted water quality measurement system (UAMS) was developed for in situ surface water quality measurement. A custom-built hexacopter was equipped with an open-source electronic sensors platform to measure the temperature, electrical conductivity (EC), dissolved oxygen (DO), and pH of water. Electronic components of the system were coated with a water-resistant film, and the hexacopter was assembled with flotation equipment. The measurements were made at thirteen sampling waypoints within a 1.1 ha agricultural pond. Measurements made by an open-source multiprobe meter (OSMM) attached to the unmanned aerial vehicle (UAV) were compared to the measurements made by a commercial multiprobe meter (CMM). Percent differences between the OSMM and CMM measurements for DO, EC, pH, and temperature were 2.1%, 3.43%, 3.76%, and <1.0%, respectively. The collected water quality data was used to interpret the spatial distribution of measurements in the pond. The UAMS successfully made semiautonomous in situ water quality measurements from predetermined waypoints. Water quality maps showed homogeneous distribution of measured constituents across the pond. The concept presented in this paper can be applied to the monitoring of water quality in larger surface waterbodies.

Keywords: water quality; in situ; remote sampling; UAV; integrated sensors

1. Introduction

Water is essential for human survival, and its quality should be monitored and protected. The safety of water resources is threatened by external factors such as industrial wastes and agricultural fertilizers. Water quality monitoring programs have been developed to preserve water quality and eliminate the contamination of water sources. The quality of water in rivers, ponds, and lakes can be evaluated by monitoring dissolved oxygen (DO), pH, temperature, and electrical conductivity (EC), which are the most commonly used indicators of impairment [1]. Low concentration of dissolved oxygen, undesirable temperature or pH, and inappropriate concentration of salinity lead to poor water quality. Periodic sampling and analysis allow one to characterize water and identify changes or trends in water quality over time. For example, pollutants carried by stormwater may include bacteria, nutrients, litter, sediment, oils, and heavy metals [2]. Data from water quality indicators can be used to create maps for the visualization of water quality distribution over a waterbody. Such maps are used by hydrologists to understand circulation in the waterbody and make predictions [3]. Through monitoring, information can be gathered to implement specific pollution prevention and remediation programs.

Streams receive point source pollutants from drainage channels, outlets from industrial plants, wastewater treatment facilities, confined animal feeding operations (CAFOs), and runoff from agricultural operations; while nonpoint source pollutant inflow occurs after rainfall or emergency overflow during a short period [4]. Nonpoint sources, including impervious surfaces such as roadways, rooftops, parking lots, and sidewalks, accumulate pollutants and convey them directly

to lakes, rivers, and estuaries [5]. Runoff that is heated up on parking lots and roadways leads to warmer-than-normal water entering nearby waterways, thereby increasing the surface water temperature. These sources can be monitored using event-controlled water samplers, automated real-time remote monitoring systems, and grab samples collected by individuals [6–8]. In addition to water sampling after a storm event, regular water sampling is necessary to identify the entry points of pollutants into surface water. For example, nutrient leaching from farm fields or pasture land into surface water has the potential to cause algal blooms [9]. The growth of dense algal blooms causes discoloration in water bodies, and can potentially result in damaging fluctuations of dissolved oxygen. Among algal blooms, blue-green algae have the genetic potential to produce toxins which are harmful to humans and animals [10,11]. Traditionally, to detect harmful changes in the waterbodies, agencies responsible for water quality monitoring collect water samples periodically and analyze them in the laboratory. These methods are costly, labor-intensive, and the measurements are not representative of the neighboring waterbodies [12]. Therefore, watershed managers face the challenge of integrating new tools for water quality monitoring, such as effect-based tools (e.g., biomarkers and bioassays) [13], automated monitoring devices [14,15], and remote sensing [16]. Remote sensing has the advantages of making measurements on a larger scale and over a long time period [12]. This allows the managers to observe the changes in water quality in coastal waters, estuaries, lakes, and reservoirs over time [12]. Despite the developments in remote sensing, most management decisions are still based on the traditional measurement methods of water sample collection and subsequent laboratory analysis [17]. In addition, data from traditional point sampling is not sufficient for identifying spatial or temporal variations in water quality, nor for forecasting for large waterbodies [17]. The integration of satellite remote sensing data with in situ measurements is necessary for making accurate and timely management decisions [12].

Autonomous underwater vehicles (AUVs) and autonomous surface vehicles (ASVs) have been developed for water quality monitoring in order to address this issue [9,18]. The autonomous vehicles that are operated in water are effective and able to conduct continuous water quality monitoring. These vehicles also have limitations and challenges. The major challenge of water quality monitoring with an underwater vehicle is the accurate positioning of the vehicle, as the Global Positioning System (GPS) cannot be used accurately when the vehicle is underwater. Because of this limitation, the AUVs must be equipped with additional navigational devices or acoustic localization systems. The ASV can automatically navigate to predefined sampling points and measure pH, DO, EC, turbidity, temperature, sensor depth, water depth, chlorophyll *a* concentration, and nitrates [9]. One of the limitations of ASVs is the difficulties in operation caused by swaying from side to side and uncertain engine-control frequencies. The ASVs and AUVs provide high spatiotemporal resolution of data and adaptive sampling due to their ability to do continuous sampling [19]. A disadvantage is the collection of biased data due to dirty and continuously-used sensor equipment.

Despite the availability of assistance from volunteers for monitoring water quality, some lakes, retired mining zones, or other waterbodies surrounded by steep and difficult terrain may not be accessible by boats [20]. In addition, lakes with cyanobacteria (blue-green algae) blooms may pose risks to humans during collection of water samples [7,21]. While AUVs, ASVs, and fixed monitoring stations are available for in situ water quality monitoring, advanced remote and autonomous in situ water sampling systems are underdeveloped [22]. The developments in unmanned aerial vehicle (UAV) technology provide new opportunities to collect water samples and to conduct in situ water quality measurements. Compared with traditional water quality monitoring methods, UAVs are relatively inexpensive, and they can be used for water quality monitoring in waterbodies that are inaccessible with boats or dangerous to field personnel.

In this study, we developed a multiprobe meter and integrated it within a hexacopter UAV for autonomous in situ water quality measurements, and verified the functionality and accuracy of the system with laboratory and field tests.

2. Materials and Methods

2.1. Design, Control, and Navigation

The primary purpose of using a UAV-assisted measurement system (UAMS) was the navigation of the UAV to the predetermined sampling points to measure the DO, EC, pH, and temperature of the water. The developed system consists of a hexacopter UAV and an open-source multiprobe meter (OSMM). We designed and built the hexacopter, developed the OSMM using off-the-market sensors and electronic components, and designed the 3D-printed cases. The design considerations for the UAV included the abilities to complete the flight mission within the allowed battery power limits, to overcome wind conditions and gusts, and to minimize crash risks that may occur due to environmental conditions or an electronic component failure; and a size large enough to carry the payload (OSMM). A hexacopter UAV was chosen to enable the carrying of relatively large payloads and overcoming wind conditions. All electronic circuits in the system were waterproofed by using a corrosion prevention spray (Corrosion-X 90102, Corrosion Technologies, Dallas, TX, USA). Flotation attachments were placed under each motor and mainframe to minimize air drag, and to increase stability during landing and takeoff. The initial hexacopter frame that was built had a hull length of 550 mm. After preliminary testing of the hexacopter with flotation attachments and the OSMM payload, the UAV was not providing a stable buoyancy in water. Therefore, the arms of the frame were lengthened with 8 mm extension plates, and this provided a more stable buoyancy in water. Thus, the total hull length of the hexacopter was 566 mm (Figure 1). The weight of the aircraft (hexacopter) was 2333 g, including the weights of the UAV frame, main battery, Electronic Speed Controllers (ESCs), motors, propellers, Pixhawk controller, GPS sensor, buzzer, safety switch, and flotation equipment. The payload had a weight of 750 g, including the weights of the OSMM components: a second battery, an Arduino board, probes, probe cables, and the protective cases for the probes and the microcontroller. The gross weight of the UAMS was 3083 g, including the weight of the aircraft and the payload.

Two batteries were used in the UAMS: one for the UAV and one for the OSMM. The main battery used to power the UAV was a 14.8 V Lithium Polymer (LiPo) battery with a 25 C discharge rate and 5000 mAh capacity (Venom, Rathdrum, ID, USA). The second battery was a 7.4 V LiPo battery with an 8 C discharge rate and 2200 mAh capacity (Venom, Rathdrum, ID, USA). The second battery was used with a battery eliminator circuit (BEC) to regulate the voltage to the microcontrollers' power specifications used for the OSMM. Using a separate battery for the OSMM allowed the operator to dismount the OSMM for standalone measurements (if needed) without the UAV being on the shore or on the boat.

(**a**) (**b**)

Figure 1. The unmanned aerial vehicle-assisted measurement system (UAMS): (**a**) prior to a flight mission; (**b**) floating on a water surface while making measurements.

The OSMM was integrated with the frame of the UAV and located on top. The electronic components of the OSMM were placed into a waterproof case to prevent water damage. The case was positioned as to maintain the center of gravity of the hexacopter. Probes were connected to the case with a BNC (Bayonet Neill-Concelman) connector, and extension cords were tied together to provide uniformity. Extension cords were 60 cm long, which determined the depth of water quality measurements. Water sampling depth may be adjusted by using longer extension cords. A custom-designed probe housing was 3D-printed and assembled to provide safeguard around the probes, to prevent the probes from getting damaged during takeoff and landing (Figure 2).

Figure 2. Custom-designed probe housing was 3D-printed with polylactic acid (PLA) material.

Control of the UAV can be accomplished either manually or autonomously. Manual control of the hexacopter was accomplished with a radio controller (RC) (Turnigy 9X, Hextronik, ChengDu, Donguan, China). Autonomous control of the hexacopter was accomplished with a Pixhawk autopilot (Pixhawk, 3DR Robotics, Berkeley, CA, USA). The Pixhawk is accompanied with a GPS receiver (3DR, Berkeley, CA, USA) and radio telemetry (3DR, Berkeley, CA, USA) for autonomous control and ground communication. The Pixhawk controller contains an MPU6000 main accelerometer and gyro, ST Micro 16-bit gyroscope, ST Micro 14-bit accelerometer/compass (magnetometer) (3DR, Berkeley, CA, USA), and MEAS barometer sensors (3DR, Berkeley, CA, USA). Mission Planner software was used to specify flight boundary, waypoints, autonomous navigation details, and to configure integrated sensors/actuators [23].

Stabilized control of a UAV is essential when flying over water surfaces. Multiple considerations must be evaluated when choosing electronic parts for these vehicles [24]. Electronic parts were chosen depending on desired payload, flight time, and compatibility. Thrust-to-weight ratio must be justified in UAV design for a stable flight. Higher thrust-producing UAVs can be designed with larger components, but this would increase costs. The major limiting factor for the UAV that we designed in-house was the cost of the motors, frames, propellers, ESCs, and battery. In this study, we used a UAV that we built for collecting water samples [25]. In the design, the payload capacity was assumed to be 400 g, which was the weight of a thief water sampler holding 130 mL of water [25]. Previous indoor flight experiments showed that the UAV can fly autonomously and continuously for 6 min while carrying a payload of 400 g [25]. These limitations were considered during OSMM construction and integration with the UAV. During the experiments, the UAMS landed on the water surface at each measurement point. Therefore, during the measurements, the main battery of the motors did not consume power, enhancing its endurance.

2.2. Accuracy Assessment

The commercial multiprobe meter (CMM) contained a portable Sension 156 meter (Hach, CO) for measuring pH and EC, and a portable HQ10 meter (Hach, Loveland, CO, USA) with DO and temperature probes. The OSMM was a combination of a water sensor node (Atlas Scientific, New York, NY, USA) and an open-source electronic platform (Arduino Mega 2560, Ivrea, Italy) (Figure 3). The water sensor node consisted of EC, DO, pH, and temperature circuits (Atlas Scientific, New York,

NY, USA), and was integrated with a microcontroller (Atmel ATmega2560, San Jose, CA, USA). The circuit was integrated with a tentacle shield (Atlas Scientific, NY, USA). The sensor readings were gathered with an Inter-Integrated Circuit (I^2C) protocol, and data was recorded in a Secure Digital Card (SD card) inserted on the shield (SunFounder, Shenzhen City, Guangdong Province, China). The advantage of an I^2C over a serial peripheral interface (SPI) is that the I^2C bus uses only two wires for multiple devices, either as a slave or a master [26]. Both the CMM and OSMM probes were calibrated in the laboratory following the manufacturers' (Atlas Scientific, NY, and Hach, CO, USA) calibration procedures.

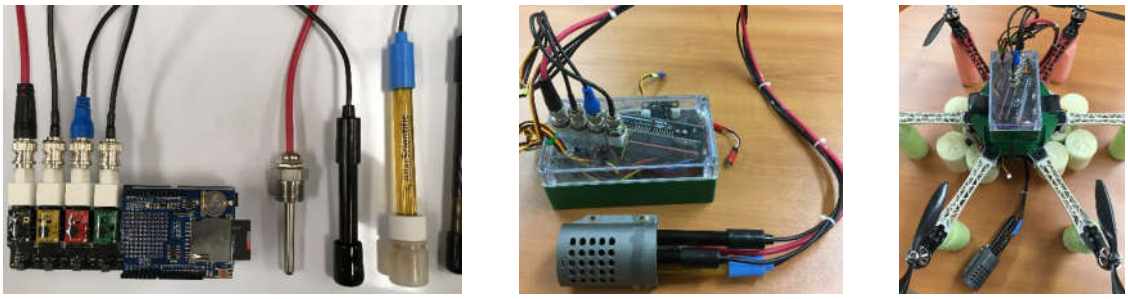

(**a**) (**b**) (**c**)

Figure 3. (**a**) The open-source multiprobe meter (OSMM) components; (**b**) placed in a waterproof case; (**c**) placed on top of the unmanned aerial vehicle (UAV).

Preliminary experiments were conducted to determine whether water quality measurements were consistent between the OSMM and the commercial multiprobe meter (CMM), before integrating the OSMM with the UAV. Both the OSMM and CMM were brought to the sampling points by kayak. To minimize the risk of the electronics of the OSMM and CMM probes getting in contact with water, water samples were collected at the predetermined sampling locations and measurements were made on the kayak. The UAMS was designed to take measurements at a depth of 60 cm. Because of this, water samples were collected with a custom-designed 3D-printed thief style sampler at a depth of 60 cm [27]. The measurements for each water quality parameter were made at the same time from two different beakers. Water samples in the beakers were manually stirred with the probe during DO measurements.

Water samples were collected from thirteen locations to verify consistency between OSMM and CMM measurements. At each location, three replicates of water samples were collected, and the average of the measurements was used in analysis. Measurements of DO, EC, pH, and temperature were made with the OSMM and CMM at each location. Of primary interest was the accuracy of the measurements made with the OSMM. A paired *t*-test analysis was conducted in Microsoft Excel (Excel 2016, Microsoft, Redmond, WA, USA) to evaluate statistical differences between the measurements of DO, EC, pH, and temperature made by the OSMM and CMM, respectively. Percent errors of each water quality parameter were calculated to determine how close the OSMM measurements were to the CMM measurements.

2.3. In Situ Data Collection with UAMS

The UAMS was launched from the shore and ascended to the flight altitude of 10 m (Figure 4). Once the UAMS had reached the waypoint in the flight mission, it descended and landed on the water. The OSMM recorded the measurements, then lifted off to the 10-m flight altitude and navigated to the next waypoint in the flight mission. A relay command was assigned to the first relay channel of the Pixhawk's auxiliary output port, to activate the data recording in OSMM. The OSMM was activated by the Pixhawk for 60 s at the sampling location. This was the time necessary for the sensors to provide stabilized measurements. The Mission Planner navigation command order that was used to

collect water at each measurement location is shown in Table 1. The "waypoint" command with 60 s delay and without latitude and longitude coordinates provided the necessary time for UAMS to take measurements [28]. During the measurements, the probes were placed in the water, and there was no stirring for the DO measurements except the mixing during the entry of the probes in water.

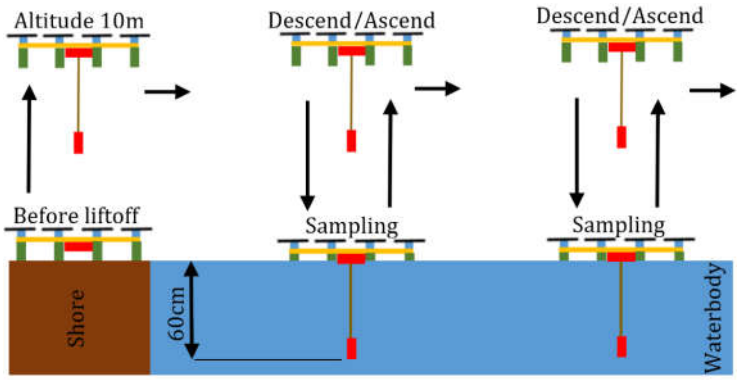

Figure 4. Applied method of water quality measurement using the UAMS.

Table 1. Autonomous navigation commands used for the UAMS mission flight.

Command Order	UAMS Position	Command	UAMS's Response	Delay (s)	Latitude	Longitude	Altitude (m)
1	Home	TAKEOFF	Take off and ascend	0	34.656951	−82.820333	10
2	Home	WAYPOINT	Navigate to WP1	0	34.656996	−82.820065	10
3	WP1	LAND	Land at WP1	0	34.656996	−82.820065	0
4	WP1	DO_SET_RELAY	Activate data recording	0	34.656996	−82.820065	0
5	WP1	WAYPOINT	Float for 60s	60	-	-	0
6	WP1	TAKEOFF	Take off and ascend	0	34.656996	−82.820065	10
7	WP1	WAYPOINT	Navigate to WP2	0	34.656884	−82.819681	10
8	WP2	LAND	Land at WP2	0	34.656884	−82.819681	0
9	WP2	DO_SET_RELAY	Activate data recording	0	34.656884	−82.819681	0
10	WP2	WAYPOINT	Float for 60s	60	-	-	0
11	WP2	TAKEOFF	Take off and ascend	0	34.656884	−82.819681	10
12	WP2	WAYPOINT	Navigate to WP3	0	34.656909	−82.819256	10

Note: These command orders were repeated for all the waypoints.

Fifteen continuous readings were made at each waypoint. The average of these measurements was taken as the water quality data for the given sampling point. Subsequently, the OSMM was switched off and the UAMS navigated to the next waypoint. The navigation path was divided into sections which included two, three, or four waypoints, depending on the distance to the launch location and available battery power.

The UAMS was designed for fully autonomous operation. In autonomous mode, the UAMS navigates to the predefined waypoint, lands on the water surface, triggers the OSMM measurements, lifts off, and navigates to the next waypoint. In addition to this, a remote-control option of the UAMS for water quality measurements was added to the system. For this purpose, a manual switch on the radio controller (RC) was designated to turn the OSMM measurements on and off remotely. The OSMM starts to record the measurements when the OSMM switch on the RC is turned on, and stops when the OSMM switch is turned off by the operator. The remote-control option of the UAMS allows the operator to conduct water quality measurements independently from autonomous UAMS control. The UAMS can be piloted manually via the RC to collect water quality data from random locations. The remote-control option allowed flexibility when the flight path was blocked by trees or when the wind speed was not suitable for safe flight.

The collected water quality data was used to create maps for visualization of water quality distribution. The data was processed in ArcMap (Esri, Redlands, CA, USA) and interpolated

using the Inverse Distance Weighted Interpolation (IDW) method [29]. Vector data in Geographic Information System (GIS) was interpolated to develop raster maps to simulate data values for intermediate locations.

2.4. Experiment Site

Both the accuracy assessment experiments of OSMM, and in situ data collection were made at Lamaster Pond at Clemson, SC. The area of the pond was 1.1 ha. The total number of measurement points on the pond and the duration of a flight mission were limited by battery power availability, and the difficulty of autonomous operation at the narrow section of the pond. Thirteen waypoints were selected randomly, with respect to the representation of the entire pond. Water depth measurements were made manually with a kayak and a marked rope at each location. The UAMS launch location and sampling waypoints are represented by circles on the map (Figure 5). The Lamaster Pond was selected as the experiment site because of its size and ease of access. The number of sampling points and their locations were selected randomly, for more stringent testing of the in situ measurement method.

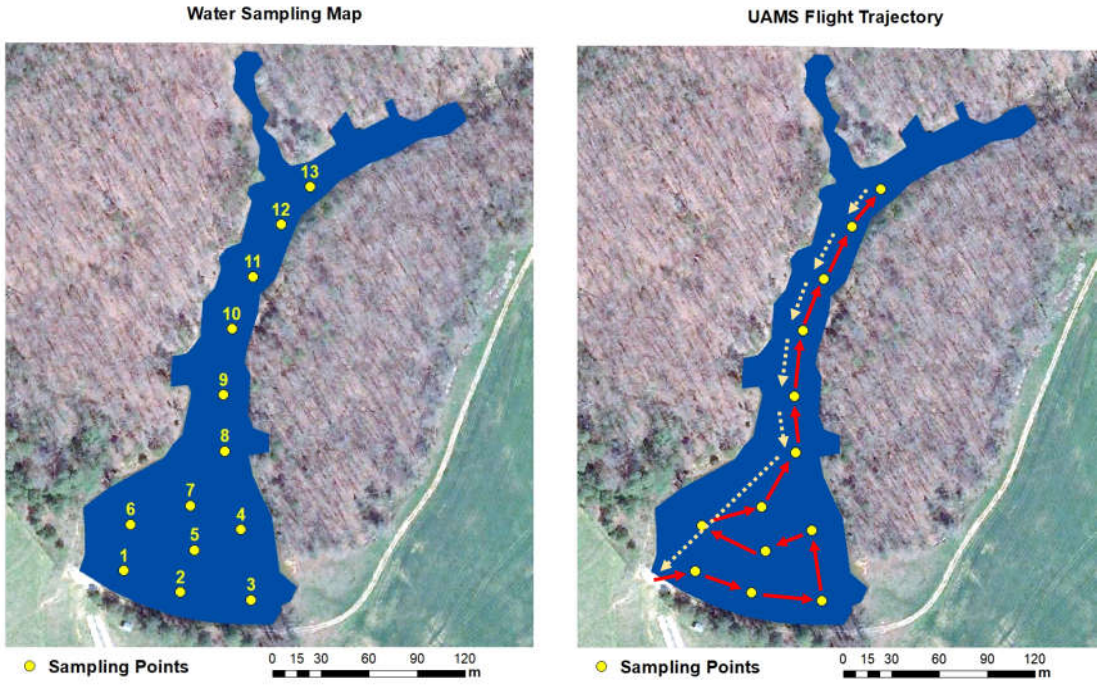

(**a**) (**b**)

Figure 5. Satellite images from Google (maps.google.com). (**a**) UAMS sampling waypoints; (**b**) Complete flight mission trajectory at Lamaster Pond, Clemson, SC. The dashed arrows on (**b**) indicate the flight path from the last waypoint to the home location.

The flight mission was divided into three sections. The first mission flight included sampling points 1, 2, 3, 4, 5, and 6. The second mission flight included sampling points 7, 8, 9, and 10. The third mission flight included sampling points 11, 12, and 13. The first and second flight missions were launched from the home location, but the third flight mission was launched from the water surface near waypoint 11. The total direct flight lengths were 256 m for the first flight, 396 m for the second, and 166 m for the third. Batteries were replaced before each flight mission. If the batteries used had had enough capacity to provide longer endurance, water sampling from all thirteen points could have been achieved in one mission flight with a total flight length of 765 m. The flight altitude was set to 10 m to minimize crash damage risks and optimize battery usage. In order to maximize battery usage, the UAMS was landed at each waypoint and the motors were shut down during in situ measurements.

3. Results

3.1. Accuracy Assessment Results

Both the OSMM and CMM probes were calibrated in the laboratory following the manufacturers' guidelines. At each measurement location, 15 measurements were made with the OSMM, providing a total of 195 data points. The CMM measurements were replicated three times at each location, providing 39 data points. A paired *t*-test was conducted to compare the differences between the OSMM and CMM measurements for each water quality parameter. In the paired *t*-test, we hypothesized that differences in the measurements made by the OSMM and CMM for each parameter, respectively, would not be statistically significant at an alpha level of 0.05.

The paired *t*-test statistics indicated that the temperature measurements made by the OSMM were significantly higher than those made by the CMM ($t(12) = 9.7$, $p < 0.001$). The paired *t*-test statistics also indicated that EC measurements made by the OSMM were significantly lower than the corresponding CMM measurements ($t(12) = 6.1$, $p < 0.001$). The percent error of the EC and temperature measurements made by the OSMM as compared with those of the CMM were 23.99% and 9.55%, respectively; whereas the differences in pH and DO between measurements made by the OSMM and CMM were not statistically significant. The average difference in DO measurements made by the OSMM and CMM was not significantly high ($t(12) = 1.34$, $p = 0.1$). There was not a significant difference in the average pH values between the OSMM and CMM measurements ($t(12) = 1.76$, $p = 0.05$). The accuracy of the DO and pH measurements made by the OSMM, relative to those made by the CMM, was 97.92% and 96.24%, respectively. Table 2 shows the summary statistics for water quality parameters obtained by the OSMM and CMM.

Table 2. Descriptive statistics for water quality parameters obtained by the OSMM and CMM.

Quality Parameter	OSMM			CMM			Difference (%)	*t* Value (DF)	*p* Value
	N	Mean	SD	N	Mean	SD			
Temp. (°C)	195	27.15	0.93	39	24.79	0.58	2.33	9.7 (12)	0.0001 ***
EC (µS/cm)	195	49.2	9.69	39	64.73	4.57	3.43	6.1 (12)	0.0001 ***
pH	195	8.43	0.86	39	8.12	0.36	3.76	1.76 (12)	0.05
DO (mg/L)	195	9.05	0.27	39	8.87	0.49	2.08	1.34 (12)	0.1

Notes: N: Number, SD: Standard deviation, DF: Degrees of freedom, Significance levels *** = $p < 0.001$

Although EC and temperature measurements were statistically different, they followed a similar pattern, as shown in Figure 6. The average difference in EC measurements (17.75 µS/cm) between those of the CMM and OSMM was added to the OSMM measurements as a correction factor. Similarly, the average difference in temperature measurements (−2.33 °C) between those of the OSMM and CMM was added to the OSMM measurements as a correction factor. These differences would be a result of the type of instruments made by different companies causing instrument error. The Hach EC probe is supplied with a meter that measures temperature with a thermistor for automatic compensation, whereas the Atlas Scientific temperature probe is a RTD (Resistance Temperature Detector). The EC measurements are corrected for sample temperature. The differences in the method of temperature measurement may be the reason for the differences in the EC measurements between the OSMM and CMM.

After applying the correction factors, the paired *t*-test statistics were conducted again for EC and temperature data. The results of the descriptive statistics is shown in Table 3. The paired *t*-test indicated that there was not a significant difference in the averages of EC measurements between the OSMM and the CMM ($t(12) = 0.87$, $p = 0.2$). The average corrected temperature values of the OSMM were not significantly different from the CMM values ($t(12) = 0.13$, $p = 0.45$). After applying the correction factors, the accuracies of the EC and temperature measurements made by the OSMM increased to 96.5% and 99.87%, respectively.

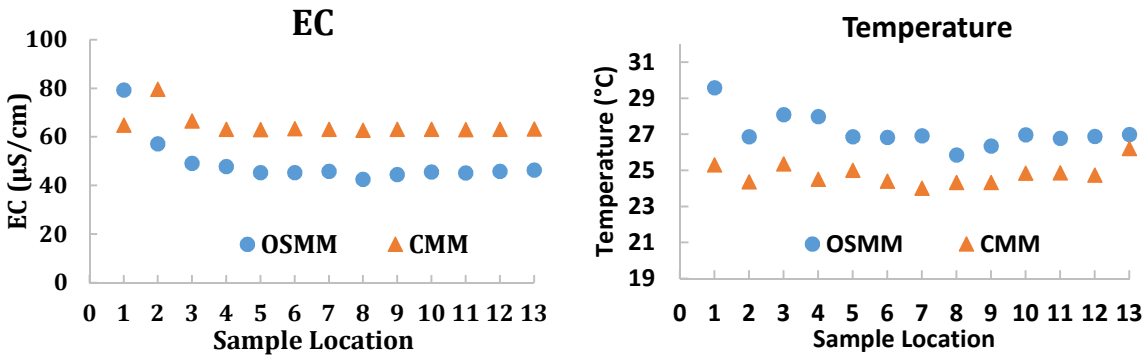

Figure 6. (**a**) Electrical conductivity (EC) and (**b**) temperature measurements, as made by the OSMM and CMM.

Table 3. Descriptive statistics for water quality parameters obtained by the OSMM and CMM, after applying correction factors to the EC and temperature measurements.

Quality Parameter	OSMM			CMM			Difference (%)	*t* Value (DF)	*p* Value
	N	Mean	SD	N	Mean	SD			
Temp. (°C)	195	24.82	0.93	39	24.79	0.58	0.13	0.13 (12)	0.45
EC (µS/cm)	195	66.95	9.69	39	64.73	4.57	3.43	0.87 (12)	0.2
pH	195	8.43	0.86	39	8.12	0.36	3.76	1.76 (12)	0.05
DO (mg/L)	195	9.05	0.27	39	8.87	0.49	2.08	1.34 (12)	0.1

Notes: N: Number, SD: Standard deviation, DF: Degrees of freedom.

3.2. In Situ Water Quality Measurements Using the UAMS

The UAMS was tested in multiple preliminary field experiments to evaluate its performance, measurement accuracy, and suitability with the proposed in situ water quality measurement method, in a variety of wind conditions and operational scenarios. All the preliminary tests and data collection experiments were conducted at Lamaster Pond in Clemson, SC. The autonomous navigation and control of the UAMS was interrupted occasionally to determine the best control method for in situ measurements. It is important to note that once the autonomous mode of the flight mission was interrupted by the operator in case of an emergency, the operator took over the control of the UAMS with the RC. The operator landed the UAMS on the water surface and manually activated the OSMM measurements. During this process, the previous sampled waypoints were removed from the flight mission using the control station, and a new flight mission was transmitted to the UAMS for autonomous navigation via radio telemetry. The operator activated the new flight mission remotely, and the UAMS continued sampling for the remaining waypoints autonomously. This process was repeated whenever the flight mission was interrupted by the operator.

The water quality parameters in Lamaster Pond were measured using the UAMS following the procedure described in Section 2.3. The data recorded on the OSMM SD card was retrieved and processed to develop surface maps for each measured parameter. Figures 7 and 8 show the manual depth measurements and the spatially interpolated data retrieved from the UAMS. The water depth at the measured locations varied between 1.22 and 4.57 m. The depth at the southeast of the pond was the deepest, whereas the north side of the pond had the most shallow depth measurements. The temperature measurements varied between 14.02 and 16.42 °C. The shallower sections of the pond had slightly higher temperatures than the deeper sections (Figure 8a). The data maps show an inverse relationship between pH and water depth (Figure 8b). As shown by the map, the pH values tended to be lower where the depth was increased. The highest pH measurements were recorded at

the north side of the pond, where the water depth was lower than in the other locations. The maps indicate an inverse relationship between DO and EC values (Figure 8c,d). In addition, the DO values decreased with increasing temperature. The variation of EC values was not high across the pond, but it tended to be higher at the southwest part of the pond. Maps provided graphical representation of the distribution of water quality parameters in the pond. These maps were useful in terms of interpreting the spatial distribution of water quality data.

Traditional in situ water quality measurement and water collection for laboratory analyses is still the preferred method used to make management decisions [12]. While these measurements provide accurate results, they do not give a spatial or temporal view of water quality over the waterbody [30]. Remote sensing techniques are being used to develop regression models between the band ratios and water quality parameters [31]. To develop accurate regression models, the remote sensing data must be verified with labor-intensive and time-consuming field experiments. UAMS-type measurement systems can be used for collecting field data and for verification of remote sensing data.

While satellite remote sensing can cover large areas, the satellite remote sensing devices scan earth surfaces systematically, and there would be a delay between passes over a given area of earth; thus, the resolution of the satellite images may not be high enough for developing regression models between the band ratios and water quality parameters [31]. Furthermore, prolonged weather conditions such as cloudiness would hinder the quality of satellite imaging. In those conditions, UAVs can be mounted with imaging sensors to collect high-resolution aerial images of relatively small waterbodies [31]. High-resolution aerial imagery would be useful for identifying hydromorphological features such as riffles, side bars, and submerged vegetation along the rives [32]. Aerial images with resolutions of less than 5 cm can only be accomplished with UAV-mounted imaging devices [32].

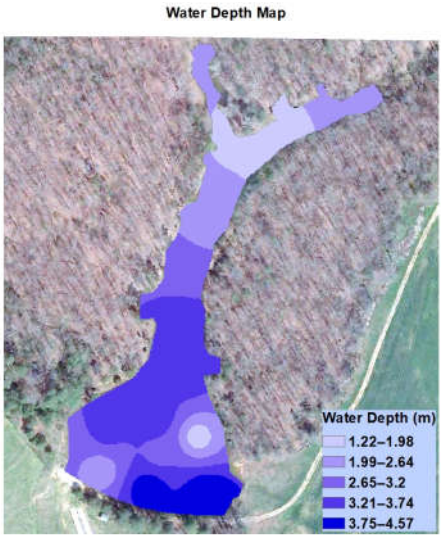

Figure 7. Spatially interpolated data from manual depth measurements.

In this study, we selected the measurement locations in a pattern to collect data from which to develop surface maps for each measured parameter. For larger waterbodies, optical and thermal sensors on UAVs, satellites, or manned aircrafts can be used as guidelines for determining the water quality measurement or water collection sampling locations [30]. Depending on the variation in aerial imagery, the number of measurement points and their locations can be determined for in situ measurements or sample collections. UAMS-type systems can also be used for water collection after natural disasters such as hurricanes and flooding [25,33]. Field personnel may not be able to collect water samples or conduct water quality measurements immediately after a disaster. In those cases, UAMS-type systems can be deployed for water sampling and water quality assessment.

Stationary sensors or sensors placed on ASVs and AUVs are often used for prolonged durations in water without being cleaned. The OSMM probes can be cleaned and maintained after every mission flight; this would eliminate problems caused by dirty and continuously-used sensor equipment.

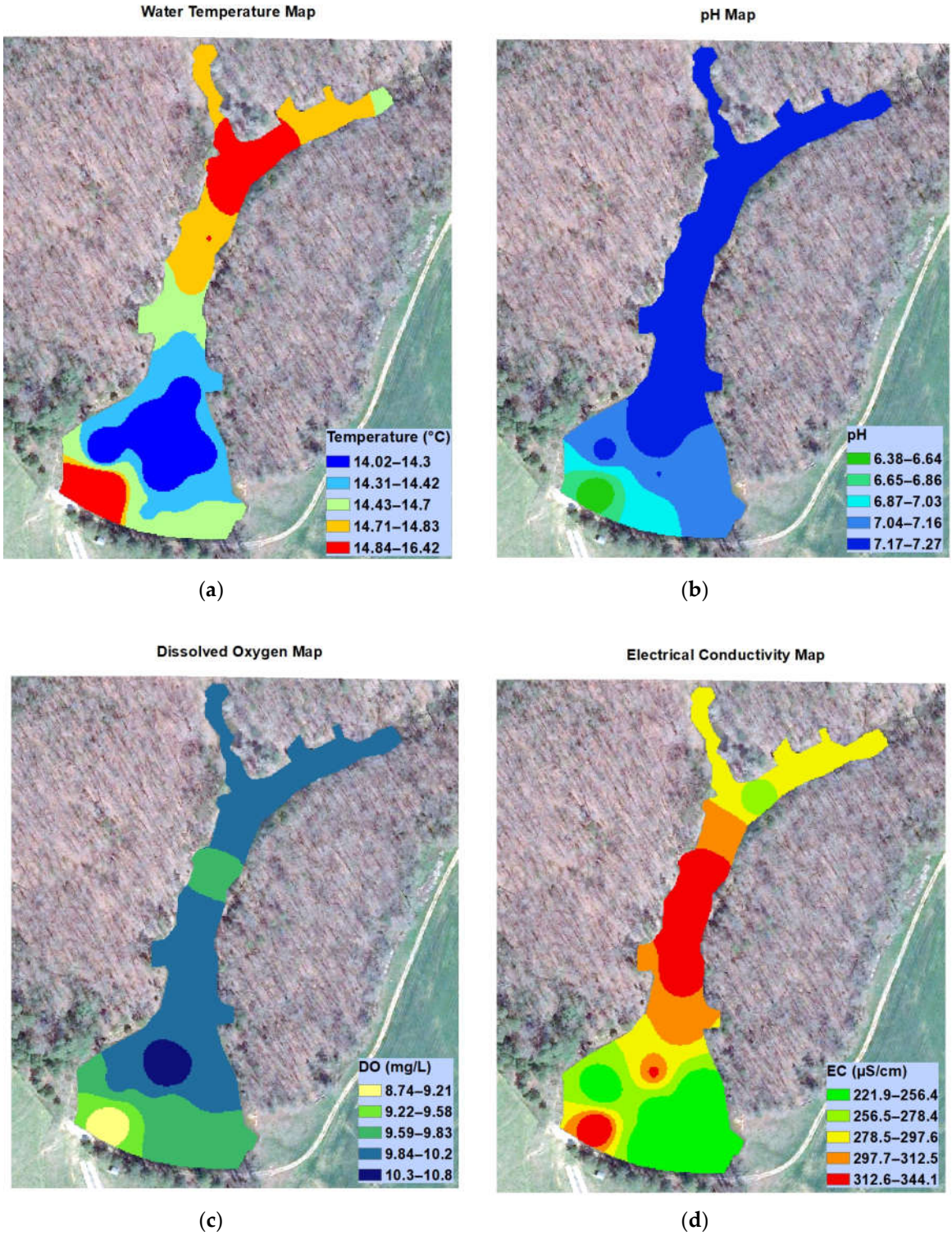

Figure 8. Spatially interpolated data from the UAMS: Water quality maps showing (**a**) water temperature, (**b**) pH, (**c**) dissolved oxygen, and (**d**) electrical conductivity.

4. Conclusions

A UAV-assisted in situ water quality measurement system (UAMS) was developed and tested. The backbone of the UAMS was the custom-built hexacopter that carried the open-source multiprobe meter (OSMM). Flotation equipment mounted under the hexacopter allowed the UAV to land on the water surface at the waypoints in the flight mission. Landing and lifting off from water surface avoided requiring the hexacopter to hover during the in situ measurements with the OSMM. This option greatly increased the endurance of the UAMS and the possible number of sampling points in each flight mission. Landing on the water surface during sampling reduced the complexity of the UAMS, by eliminating the need to use additional sensors for safe hovering for taking measurements at a precise depth. The developed prototype UAMS was waterproof, lightweight, and fully functional for collecting georeferenced temperature, electrical conductivity (EC), dissolved oxygen (DO), and pH data from a 1.1 ha agricultural pond.

The developed prototype UAMS can be used to collect field data for the development of algorithms for water quality assessment with satellite remote sensing. UAMSs can also be used for conducting field measurements at inaccessible or dangerous waterbodies. Another important contribution of the UAMS would be in rapid water quality measurements after natural disasters such as flooding and hurricane events. The major limiting factor for the UAMS is flight duration. Advancements in battery technology and optimal UAV designs can increase the endurance of the UAMS. Future research activities will focus on the development of a new UAMS for smart water sampling, based on the OSMM measurements.

Acknowledgments: The research was funded by Clemson University, Clemson, South Carolina, U.S.A. We thank the anonymous reviewers and the editor-in-chief for their constructive comments, which helped to improve this article.

Author Contributions: Cengiz Koparan created the conceptual designs and prototypes of the water sampling mechanism, developed the UAMS, conducted field experiments, analyzed the data, and wrote the draft manuscript. Bulent Koc conceptualized the idea of UAV-assisted water quality monitoring, supervised the research, and led the writing of this paper. Charles Privette and Calvin Sawyer provided their expertise in water quality assessment, provided the laboratory instruments, provided feedback on the data collection and analyses, and helped producing the final version of the paper.

Conflicts of Interest: The authors declare no conflict of interest.

References

1. Xu, Z.; Dong, Q.; Otieno, B.; Liu, Y.; Williams, I.; Cai, D.; Li, Y.; Lei, Y.; Li, B. Real-time in situ sensing of multiple water quality related parameters using micro-electrode array (mea) fabricated by inkjet-printing technology (ipt). *Sens. Actuators B Chem.* **2016**, *237*, 1108–1119. [CrossRef]
2. Thomas, K.V.; Hurst, M.R.; Matthiessen, P.; Sheahan, D.; Williams, R.J. Toxicity characterisation of organic contaminants in stormwaters from an agricultural headwater stream in south east england. *Water Res.* **2001**, *35*, 2411–2416. [CrossRef]
3. Kaizu, Y.; Iio, M.; Yamada, H.; Noguchi, N. Development of unmanned airboat for water-quality mapping. *Biosyst. Eng.* **2011**, *109*, 338–347. [CrossRef]
4. Liu, R.; Xu, F.; Zhang, P.; Yu, W.; Men, C. Identifying non-point source critical source areas based on multi-factors at a basin scale with swat. *J. Hydrol.* **2016**, *533*, 379–388. [CrossRef]
5. Ma, Y.; Egodawatta, P.; McGree, J.; Liu, A.; Goonetilleke, A. Human health risk assessment of heavy metals in urban stormwater. *Sci. Total Environ.* **2016**, *557–558*, 764–772. [CrossRef] [PubMed]
6. Neumann, M.; Liess, M.; Schulz, R. A qualitative sampling method for monitoring water quality in temporary channels or point sources and its application to pesticide contamination. *Chemosphere* **2003**, *51*, 509–513. [CrossRef]
7. Glasgow, H.B.; Burkholder, J.M.; Reed, R.E.; Lewitus, A.J.; Kleinman, J.E. Real-time remote monitoring of water quality: A review of current applications, and advancements in sensor, telemetry, and computing technologies. *J. Exp. Mar. Biol. Ecol.* **2004**, *300*, 409–448. [CrossRef]

8. Weiss, P.T.; Erickson, A.J.; Gulliver, J.S.; Hozalski, R.M.; Mohseni, O.; Herb, W.R. *Stormwater Treatment: Assessment and Maintenance*; University of Minnesota, st. Anthony Falls Laboratory: Minneapolis, MN, USA, 2010.
9. Blaas, H.; Kroeze, C. Excessive nitrogen and phosphorus in european rivers: 2000–2050. *Ecol. Indic.* **2016**, *67*, 328–337. [CrossRef]
10. McGowan, S. Chapter 2—Algal blooms a2—Shroder, john f. In *Biological and Environmental Hazards, Risks, and Disasters*; Sivanpillai, R., Ed.; Academic Press: Boston, MA, USA, 2016; pp. 5–43.
11. Van der Merwe, D. Chapter 31—Cyanobacterial (blue-green algae) toxins a2—Gupta, ramesh c. In *Handbook of Toxicology of Chemical Warfare Agents*, 2nd ed.; Academic Press: Boston, MA, USA, 2015; pp. 421–429.
12. Schaeffer, B.A.; Schaeffer, K.G.; Keith, D.; Lunetta, R.S.; Conmy, R.; Gould, R.W. Barriers to adopting satellite remote sensing for water quality management. *Inter. J. Remote Sens.* **2013**, *34*, 7534–7544. [CrossRef]
13. Wernersson, A.-S.; Carere, M.; Maggi, C.; Tusil, P.; Soldan, P.; James, A.; Sanchez, W.; Dulio, V.; Broeg, K.; Reifferscheid, G.; et al. The european technical report on aquatic effect-based monitoring tools under the water framework directive. *Environ. Sci. Eur.* **2015**, *27*, 7. [CrossRef]
14. Winkelbauer, A.; Fuiko, R.; Krampe, J.; Winkler, S. Crucial elements and technical implementation of intelligent monitoring networks. *Water Sci. Technol.* **2014**, *70*, 1926–1933. [CrossRef] [PubMed]
15. Winkler, S.; Zessner, M.; Saracevic, E.; Fleischmann, N. Intelligent monitoring networks—Transformation of data into information for water management. *Water Sci. Technol.* **2008**, *58*, 317–322. [CrossRef] [PubMed]
16. Tyler, A.N.; Hunter, P.D.; Carvalho, L.; Codd, G.A.; Elliott, J.A.; Ferguson, C.A.; Hanley, N.D.; Hopkins, D.W.; Maberly, S.C.; Mearns, K.J.; et al. Strategies for monitoring and managing mass populations of toxic cyanobacteria in recreational waters: A multi-interdisciplinary approach. *Environ. Health* **2009**, *8*, S11. [CrossRef] [PubMed]
17. Gholizadeh, M.; Melesse, A.; Reddi, L. A comprehensive review on water quality parameters estimation using remote sensing techniques. *Sensors* **2016**, *16*, 1298. [CrossRef] [PubMed]
18. Karimanzira, D.; Jacobi, M.; Pfuetzenreuter, T.; Rauschenbach, T.; Eichhorn, M.; Taubert, R.; Ament, C. First testing of an auv mission planning and guidance system for water quality monitoring and fish behavior observation in net cage fish farming. *Inf. Proc. Agric.* **2014**, *1*, 131–140. [CrossRef]
19. Dunbabin, M.; Grinham, A.; Udy, J. An autonomous surface vehicle for water quality monitoring. In Proceedings of the 2009 Australasian Conference on Robotics and Automation (ACRA), Sydney, Australia, 2–4 December 2009; Australian Robotics and Automation Association: Sydney, Australia, 2009; pp. 1–6.
20. Peters, C.B.; Zhan, Y.; Schwartz, M.W.; Godoy, L.; Ballard, H.L. Trusting land to volunteers: How and why land trusts involve volunteers in ecological monitoring. *Biol. Conserv.* **2017**, *208*, 48–54. [CrossRef]
21. Partyka, M.L.; Bond, R.F.; Chase, J.A.; Atwill, E.R. Monitoring bacterial indicators of water quality in a tidally influenced delta: A sisyphean pursuit. *Sci. Total Environ.* **2017**, *578*, 346–356. [CrossRef] [PubMed]
22. Ravalli, A.; Rossi, C.; Marrazza, G. Bio-inspired fish robot based on chemical sensors. *Sens. Actuators B Chem.* **2017**, *239*, 325–329. [CrossRef]
23. Ardupilot. Installing Mission Planner. Available online: http://ardupilot.org/planner/docs/common-install-mission-planner.html (accessed on 25 May 2017).
24. Gupta, A.K.; Jha, V.; Gupta, V.K. Design and development of remote controlled autonomous synchronic hexaroter aerial (asha) robot. *Proced. Technol.* **2014**, *14*, 51–58. [CrossRef]
25. Koparan, C.; Bulent Koc, A. Unmanned aerial vehicle (uav) assisted water sampling. In *2016 ASABE Annual International Meeting*; ASABE: St. Joseph, MI, USA, 2016; p. 1.
26. Lynch, K.M.; Marchuk, N.; Elwin, M.L. Chapter 13–i2c communication. In *Embedded Computing and Mechatronics with the Pic32*; Newnes: Oxford, MS, USA, 2016; pp. 191–211.
27. Koparan, C.; Koc, A.B. Unmanned Aerial Vehicle (Uav) Assisted Water Sampling. In Proceedings of the 2016 ASABE Annual International Meeting, Orlando, FA, USA, 17–20 July 2016; American Society of Agricultural and Biological Engineers: St. Joseph, MI, USA, 2016; p. 1.
28. Ardupilot. Mavlink Mission Command Messages. Available online: http://ardupilot.org/planner/docs/common-mavlink-mission-command-messages-mav_cmd.html (accessed on 10 December 2017).
29. Ahmad, H.R.; Aziz, T.; Rehman, Z.R. Saifullah. Chapter 15—Spatial mapping of metal-contaminated soils a2—hakeem, khalid rehman. In *Soil Remediation and Plants*; Sabir, M., Öztürk, M., Mermut, A.R., Eds.; Academic Press: San Diego, CA, USA, 2015; pp. 415–431.

30. Ritchie, J.C.; Zimba, P.V.; Everitt, J.H. Remote sensing techniques to assess water quality. *Photogramm. Eng. Remote Sens.* **2003**, *69*, 695–704. [CrossRef]
31. Su, T.-C.; Chou, H.-T. Application of multispectral sensors carried on unmanned aerial vehicle (uav) to trophic state mapping of small reservoirs: A case study of tain-pu reservoir in kinmen, taiwan. *Remote Sens.* **2015**, *7*, 10078–10097. [CrossRef]
32. Rivas Casado, M.; Ballesteros Gonzalez, R.; Wright, R.; Bellamy, P. Quantifying the effect of aerial imagery resolution in automated hydromorphological river characterisation. *Remote Sens.* **2016**, *8*, 650. [CrossRef]
33. Ore, J.-P.; Elbaum, S.; Burgin, A.; Detweiler, C. Autonomous aerial water sampling. *J. Field Robot.* **2015**, *32*, 1095–1113. [CrossRef]